



MiR-934 Exacerbates Malignancy of Gastric Cancer Cells by Targeting ZFP36

Zhicheng Pan, Huazhong Yun, Yun Xiao, Fei Tong, Guodong Liu, *Ge Zhang, *Jianbo Han

General Surgery Department, Nanjing Red Cross Hospital, Nanjing City, Jiangsu Province, 210000, China

*Corresponding Authors: Email: hanjianbo1982@163.com, gezhang0307@163.com

(Received 18 Dec 2022; accepted 24 Feb 2023)

Abstract

Background: In order to explore new targets for the treatment of gastric cancer (GC), we investigated the regulatory mechanism of miR-934 in the malignant phenotype of gastric cancer.

Methods: The miRNA and mRNA expressions were determined by RT-qPCR, and protein levels were quantified by western blotting assay. Malignancy of AGS cell line was evaluated by MTT, flow cytometry, wound healing and Transwell assays. The putative binding site between miR-934 and ZFP36 was validated using luciferase reporter assay. Immunohistochemistry (IHC) assay was used to visualize the ZFP36-positive cells in the xenograft sections. All experiments were conducted in General Surgery Laboratory of Nanjing Red Cross Hospital Jiangsu Province, China from June 2019 to June 2021.

Results: GC tissues and cell lines showed notably higher levels of miR-934. Overexpression of miR-934 promoted cell viability, migration and invasion, while inhibited cell apoptosis of GC cells. ZFP36 was predicted and verified to be the target of miR-934 and low protein levels of ZFP36 were observed in GC tissues. The ZFP36 protein expressions were suppressed by miR-934 overexpression, while were facilitated by miR-934 inhibition. Furthermore, the carcinogenic functions of miR-934 were partially reversed after ZFP36 overexpression. The results of in vivo experiments further demonstrated that miR-934 promoted tumor growth and repressed the protein expression of ZFP36.

Conclusion: miR-934 served as a tumor promoter in GC via targeting ZFP36, and ZFP36 overexpression could efficiently relieve malignant phenotypes caused by miR-934, which prompted an exploitable molecular target for GC treatment.

Keywords: Gastric cancer; Microna-934; Cell growth; Cell metastasis

Introduction

Gastric cancer (GC) is a tumor of the digestive tract induced by malignant gastric epithelium mucosa (1). The WHO statistics show that about 950,000 people are newly diagnosed as GC worldwide in 2012, accounting for 7.8% of the

total morbidity of malignant tumors (2). Only inconspicuous clinical symptoms emerge at the early stages of GC, which causes most GC patients were diagnosed at the advanced stages (3,4).



For the treatment of GC, surgery is currently the mainstay, along with comprehensive treatment plans including chemotherapy, radiotherapy and immunotherapy (5). However, the insidious onset and limited diagnostic methods of GC cause many GC patients to miss the best opportunity for surgery when they are diagnosed (6). With the introduction of "precision medicine" and the development of targeted drugs, targeted therapy is much accounted of GC. For example, the HER2-targeted Herceptin and the tyrosine kinase inhibitor (TKI) Apatinib can significantly improve the survival and prognosis of advanced GC patients (7). Whereas, the development of targeted therapy for GC is still in its infancy, and the targeting molecules currently employed in clinics are far from enough.

To date, microRNA (miRNA) has become a hot spot for oncology (8-10). miRNAs are a type of small non-coding RNA with a length of about 22 nucleotides (11). Commonly, miRNAs regulate gene expression via complementary binding to the 3'-UTR of mRNAs (12). miRNAs regulate about 30% of human genome genes and play vital roles in cell proliferation, cell apoptosis, and cell metastasis (13). Hence, aberrant expressions of miRNAs will impact a series of cellular metabolism in tumors. miRNAs are difunctional factors in regulating tumor progression and participate in the occurrence, development and metastasis of different cancers (13). For example, miRNA-339-5p is downregulated in GC and it inhibits the progression of GC by negatively regulating ALKBH1 (14). miR-4317 suppresses the proliferation of GC cells partly through targeting ZNF322 (15). Reversely, miR1835p.1 is proved to promote cell growth and metastasis via targeting TPM1 and deactivating the Bcl2/P53 signaling pathway in GC (16). Except for regulating cell metabolism, miRNAs can also change the radiosensitivity and chemosensitivity of the target cells (17). Therefore, in-depth study of the function of miRNA and its target genes greatly contributes to clarify the molecular mechanism of GC and may provide valuable molecular targets. miR-934 has been reported to be an oncogene in

several tumors (18-23), while the role remains unclear in GC.

In the present work, we designed to explore whether miR-934 exerted carcinogenic role in GC and screened out a target gene of miR-934 to further investigate the underlying regulatory mechanism of miR-934.

Materials and Methods

Collection of clinical samples

The GC tissues (n=16) and the paired paracarcinoma tissues (n=16) were collected from the biobank of the Nanjing Red Cross Hospital, Jiangsu Province, China. The samples were resected from the GC patients who received surgery in the hospital from June 2019 to June 2021. All samples were immediately stored in lipid nitrogen and pathological examinations were conducted after surgery. Patients underwent chemotherapy, radiotherapy or immunotherapy was excluded from this study.

All the patients were informed, signed consents were obtained from every patients, and approval was obtained from the Ethics Committee of Nanjing Red Cross Hospital, Jiangsu Province. All operations were declared to strictly observe the Declaration of Helsinki.

Cell culture and transfection

GES-1, KATO, 23132/87, AGS, HGC-27, OCUM-1, NUGC-4 (Cobioer Biotech Co., Ltd.) and 4-1st (Otwo Biotech Co., Ltd.) cell lines were cultured in DMEM with 10% FBS, 1% penicillin and streptomycin (all obtained from Solarbio Science & Technology Co., Ltd.) at 37 °C and 5% CO₂, respectively. After the cell confluence reached 70%-80%, cells were trypsinized for subculture.

AGS cells in were plated into a 96-well plate and transfected with 50 nM miR-934 mimic, miR-934 inhibitor, pcDNA3.1/ZFP36, or negative control (GenePharma Co., Ltd.) using Lipofectamine[®] 3000 reagent (Invitrogen). The sequences of miR-934 inhibitor and mimic are listed in Table 1.

Table 1: Sequences of primers and probes

<i>miR-934 inhibitor</i>	5'-CCAGUGUCUCCAGUAGUAGACA-3'
<i>miR-934 mimic</i>	5'-UGUCUACUACUGGAGACACUGG-3'
<i>miR-934</i>	forward 5'-GCCTAGAAACATCCTCCCGG-3' reverse 5'-AGGCCATGTGTCTGGTTCG-3'
<i>ZFP36</i>	forward 5'-GACTGAGCTATGTCGGACCTT-3' reverse 5'-GAGTTCGTCCTTGTATTTGGGG-3'
<i>GAPDH</i>	forward 5'-ACCCACTCCTCCACCTTTGAC-3' reverse 5'-TGTTGCTGTAGCCAAATTCGTT-3'
<i>U6</i>	forward 5'-CTCGCTTCGGCAGCACATATACT-3' reverse 5'-ACGCTTCACGAATTTGCGTGTTC-3'

Real-time quantitative polymerase chain reaction (RT-qPCR)

RNAs from cells and gastric tissues were extracted by TRIzol® (Invitrogen). BioSci® WitEnzy First-Strand cDNA Synthesis Kit (8072031) was applied to conduct reverse transcription prior to amplification. Then, BioSci® WitEnzy 2×SYBR Green qPCR Master Mix ROX Reference Dye (807302X) was used to conduct amplification on the 96 Well Real Time Fluorescent Quantitative Thermal Cycler PCR Machine (Suzhou Molarray Biotech Co., Ltd.). GAPDH was the loading control of mRNA, and U6 was for miRNA, respectively. Relative expressions of the RNAs were assessed following $2^{-\Delta\Delta C_t}$ method. Sequences of the primers were showed in Table 1.

MTT assay

AGS cells were plated into a 96-well plate (1×10^4 cells/well) and incubated at 37 °C and 5% CO₂. MTT reagent (8028; ScienCell Research Laboratories, Inc.) was added to the plate (10 µl/well) and incubated for 4 h, followed by dimethyl sulfoxide solution (DMSO; 100 µl/well; Macklin Biochemical Co., Ltd.). The optical densities were measured using a CMax Plus Microplate Reader (Molecular Devices) at the wavelength of 490 nm.

Flow cytometry assay

Annexin V-iFluor 488 + PI Apoptosis Detection Kit (CM001-100D; Chamot Biotech Co., Ltd.) was used to label the apoptotic cells following the anufacture's instruction. Briefly, AGS cells were trypsinized and rinsed twice with PBS buffer.

1×10^5 cells were resuspended and incubated with 5 µl of Annexin V-iFluor 488 and 5µl of PI for 15 min under dark. Subsequently, apoptotic cells were counted by MACSQuant® Analyzer 16 (Miltenyi Biotec).

Wound healing assay

5×10^5 AGS cells were inoculated into a 6 well plate and cultured at 37°C in 5% CO₂. Then, a wound was scraped into the cell monolayer. The wells were rinsed by PBS to remove the unadherent cells. Serum-free DMEM was added into the plate and cultured for 24 h. Wound images were observed and photographed at the beginning and ending time points under a microscope.

Cell invasion assays

The cells were cultured in serum-free DMEM (5×10^4 cells/ml) for 24 h. Matrigel (BD Biosciences) was previously coated onto transwell chambers (3422; Corning), which were inserted in a 24-well plate. The starved cells and DMEM containing 20% FBS were added into the upper chambers and lower chambers, respectively. After culture for 48 h, the invaded cells were fixed 100% methanol and stained with 0.1% crystal violet. Five visual fields were selected and captured under a light microscope.

Luciferase reporter assay

The wild or mutant type 3'-UTR sequence of ZFP36 was cloned into the luciferase reporter vectors (General Biotech Co., Ltd.) to establish the WT- and MUT-luciferase reporter plasmids.

The plasmids and miR-934 mimic/inhibitor were transfected into AGS cells and incubated for 24 h. After that, cell lysate was collected to detect the luciferase activities using the Luc-Pair™ Firefly Luminescence HS Assay Kit (LF007; GeneCopoeia Inc.). Luciferase activity of *Renilla* was used for normalization.

Western blotting assay

Total proteins from the cells and gastric tissues were extracted using the Minute™ Total Protein Extraction Kit for Animal Cultured Cells/Tissues (SN-002; Invent Biotech Inc.) and quantified by a BCA Protein Quantification Kit (E112-01; Vazyme Biotech Co., Ltd.). The detailed experiment process was carried out following the previous method (16). Primary antibodies were anti-ZFP36 (1:500; FNab09623) and anti-GAPDH (1:1000; FNab03342), and secondary antibody was streptavidin-goat anti-human IgG (H+L) (1:5000; FNSA-0049; all from Wuhan Fine Biotech Co., Ltd.).

Xenograft assay

All animal experiments were performed under the approval of the animal ethics committee of Red Cross Hospital of Nanjing. BLAB/c male nude mice (n=10; six weeks) were purchased from GemPharmatech Biotech Co., Ltd. and raised in the standard environment (24). 2×10^6 AGS cells stably expressing miR-934 were injected into the axilla of the nude mice to induce the xenografts. The tumor volume was measured at day 10, 15, 20 and 25. After induction for 25

days, solid tumors were excised and weighed after the mice were sacrificed by intravenous injection of 150 mg/kg pentobarbital.

Immunohistochemistry (IHC)

The paraffin sections of xenografts were torrefied, dewaxed and rehydrated. After antigen retrieval, the sections were blocked by 0.3% Triton X-100 (T8200; SolarBio) and incubated with rabbit anti-ZFP36 (1:100; FNab09623) primary antibody for 2 h and followed by incubation with anti-IgG. DAB developing kit (IHC0007; both from Wuhan Fine Biotech Co., Ltd.) was used to develop the sections following the manufacturer's instructions.

Statistics

Each experiment was performed for triplication. Data were analyzed by GraphPad Prism (version 8.0.1.244, GraphPad Software Inc.). The data were presented as mean \pm SD. Student t-test or ANOVA with Tukey's post hoc test was applied for the two-group or multiple group comparison. $P < 0.05$ was deemed as significant difference.

Results

miR-934 was upregulated in the GC tissues and cell lines

Through miRDB, miRWalk, Starbase and TargetScan database analysis, we found that miR-934 is likely to be related to the occurrence and development of gastric cancer (Fig. 1A).

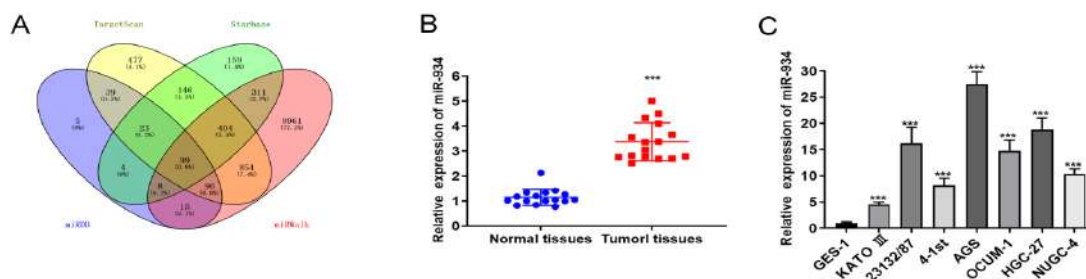


Fig. 1: miR-934 was upregulated in the GC tissues and cell lines. (A) Venn diagram of the target genes predicted by miRDB, miRWalk, Starbase and TargetScan. (B) The expression levels of miR-934 were detected in the GC tissues (n=16) and adjacent normal tissues (n=16) using RT-qPCR. (C) The expression levels of miR-934 in normal human gastric epithelial cell line (GES-1) and GC cell lines (KATO III, 23132/87, 4-1st, AGS, OCUM-1, HGC-27, NUGC-4). *** $P < 0.001$. GC, gastric cancer

we examined the expression levels of miR-934 in the GC tissues and cell lines. A markedly higher level of miR-934 was observed in the GC tissues (Fig. 1B). Meanwhile, the expression levels of miR-934 in seven GC cell lines were significantly increased than that of normal human gastric cells (GES-1) (Fig. 1C).

miR-934 positively regulated cell viability, migration and invasion of AGS cells

miR-934 mimic prominently increased the expression level of miR-934, while miR-934 inhibitor decreased it in AGS cells (Fig. 2A). Cell via-

bility was enhanced after miR-934 mimic transfection, but opposite result was observed in the miR-934 inhibitor transfection AGS cells (Fig. 2B). Cell apoptosis rates of AGS cells underwent miR-934 overexpression (OE) or inhibition exhibited the reverse trends with cell viability (Fig. 2C). Furthermore, both relative migrated distance (Fig. 2D) and invaded cell number (Fig. 2E) of AGS cells was notably promoted by miR-934 mimic, while suppressed by miR-934 inhibitor. To sum up, the results above suggested the carcinogenic role of miR-934.

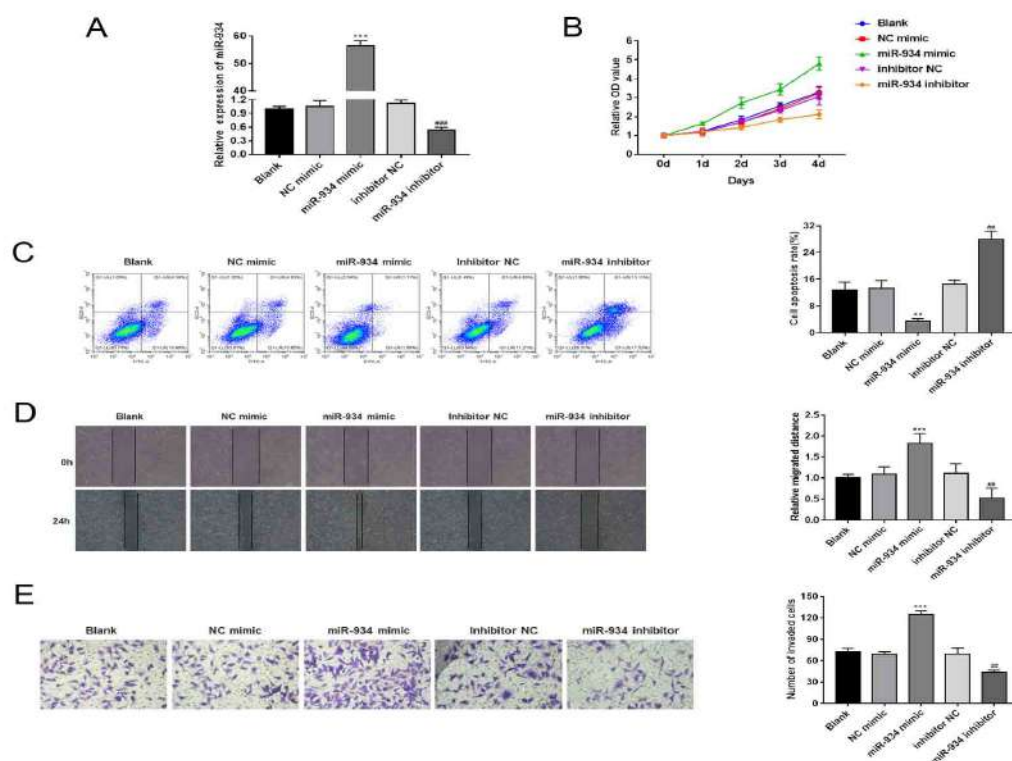


Fig. 2: miR-934 positively regulated the aggressive behaviors of AGS cells. (A) The expression levels of miR-934 of AGS cells were determined after transfected with miR-934 mimic or inhibitor. (B) OD values were measured 0, 1, 2, 3 and 4 d after conducting MTT assay. (C) Cell apoptosis of AGS cells was examined by flow cytometry assay. (D) Wound healing assay was performed to assess cell migration of AGS cells. (E) Transwell assay was carried out to evaluate cell invasion of AGS cells. Invaded cells were counted under five random views. Each assay was repeated thrice. $**P < 0.01$, miR-934 mimic vs. NC mimic; $***P < 0.001$, vs. NC mimic; $##P < 0.01$, vs. inhibitor NC; $###P < 0.001$, vs. inhibitor NC. OD, optical density; NC, negative control

miR-934 targeted for ZFP36

As Fig. S1 displayed, 99 target genes were jointly predicted by the four online database, including

miRDB, Starbase, miRWalk and TargetScan. Subsequently, UALCAN (<http://ualcan.path.uab.edu/analysis-mir.html>)

was utilized to analyze the expressions of the target genes in GC to screened out the significantly downregulated genes. Among the downregulated genes, ZFP36 was noted due to the widely reported anti-tumor characteristic (25-28). As Fig. 3A showed, miR-934 mimic significantly reduced the luciferase activity of ZFP36 WT, which was elevated by miR-934 inhibitor. However, the luciferase activity in ZFP36 MUT group was not influenced by miR-934 mimic or inhibitor. These results demonstrated the binding of miR-934 and

ZFP36. The mRNA levels of ZFP36 showed no statistical difference between GC tissues and normal tissues (Fig. 3B); whereas, the protein expression levels of ZFP36 exhibited distinct reductions in the tumor tissues (Fig. 3C and D). In addition, miR-934 mimic could observably inhibit the protein expression of ZFP36, while miR-934 inhibitor enhanced ZFP36 protein expression (Fig. 3E and F). Collectively, the findings unveiled that miR-934 inhibited the expression of ZFP36 by suppressing mRNA translation.

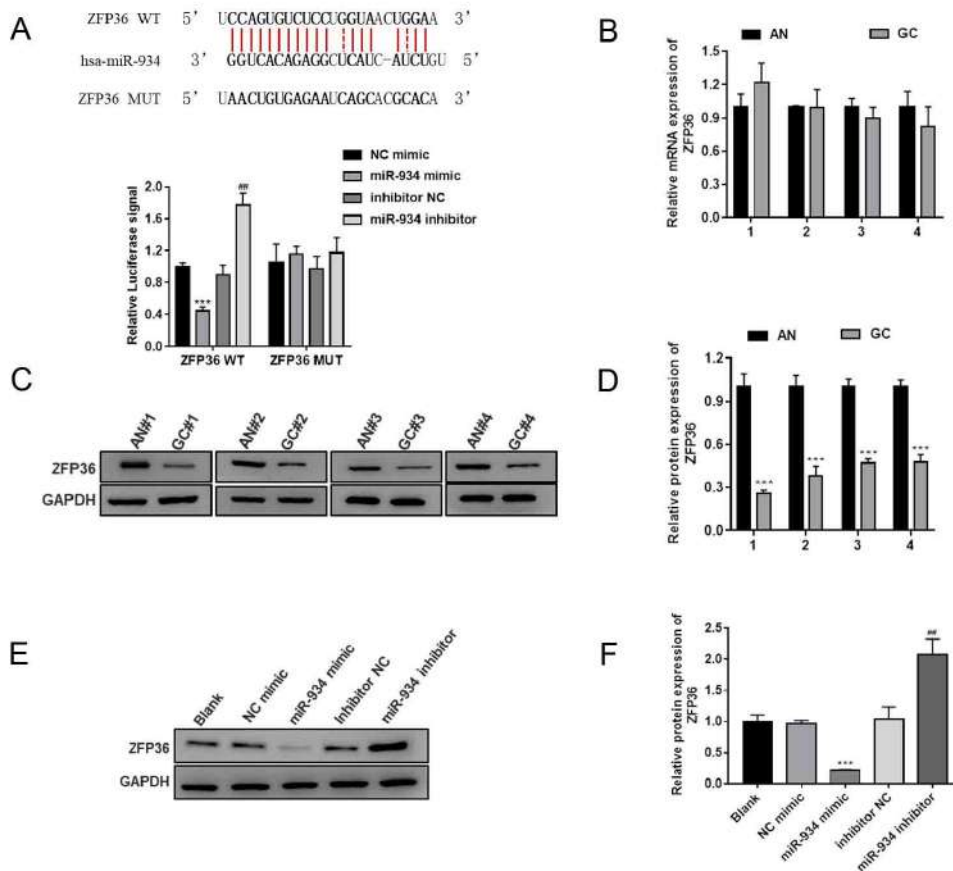


Fig. 3: ZFP36 was the target of miR-934. (A) Luciferase reporter assay was conducted to verify the binding site between miR-934 and ZFP36. (B) The relative mRNA and protein (C and D) expression levels of ZFP36 were determined in tumor tissues (n=4) and normal tissues (n=4). (E and F) The protein expression levels of ZFP36 were detected in AGS cells transfected with miR-934 mimic or inhibitor using western blotting assay. Each assay was repeated thrice. ****P* < 0.001, vs. NC mimic or AN; ##*P* < 0.01, vs. inhibitor NC; AN, adjacent normal tissues; GC, gastric cancer tissues

Restoration of ZFP36 relieved the malignant behaviors of GC cells promoted by miR-934

ZFP36 protein expression was markedly reduced after miR-934 overexpression. Moreover, ZFP36 OE could prominently promote the protein level of ZFP36 and notably ameliorated the inhibitory

effect of miR-934 mimic on ZFP36 expression (Fig. 4A). Functional experiments revealed that ZFP36 OE significantly suppressed cell viability (Fig. 4B), migration (Fig. 4C) and invasion (Fig. 4D), while accelerated cell apoptosis, reversing the carcinogenic function of miR-934.

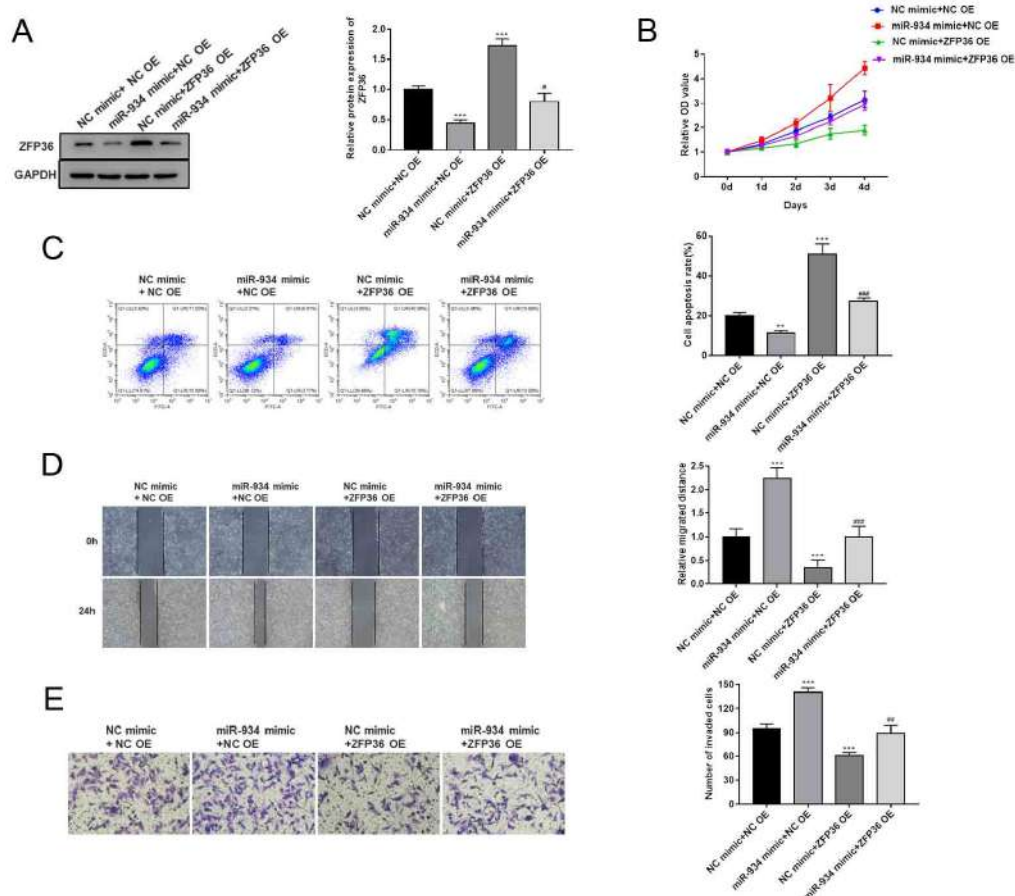


Fig. 4: Overexpression of ZFP36 partially reversed the function of miR-934. (A) The protein expressions of ZFP36 in AGS cells were examined after transfection of miR-934 mimic and/or pcDNA3.1/ZFP36. (B) Cell viabilities of AGS cells were measured after 0, 1, 2, 3 and 4 d of transfection. (C) Cell apoptosis, (D) migration and (E) invasion were analyzed in AGS cells underwent the indicated transfections. Each assay was repeated thrice. ** $P < 0.01$, vs. NC mimic+NC OE; *** $P < 0.001$, vs. NC mimic+NC OE; # $P < 0.05$, vs. miR-934 mimic+NC OE; ### $P < 0.01$, vs. miR-934 mimic+NC OE; ### $P < 0.001$, vs. miR-934 mimic+NC OE. NC, negative control; OE, overexpression

miR-934 deteriorated the malignant phenotype of xenografts

The onco-role of miR-934 was ulteriorly investigated in the xenograft mice (Fig. 5A). Tumor growth was promoted by miR-934 as evidenced by the markedly increased tumor volume (Fig.

5B) and weight (Fig. 5C). Additionally, the protein expression level of ZFP36 was notably reduced by miR-934 in the xenografts (Fig. 5D), which was also observed in the IHC images of the xenograft section (Fig. 5E).

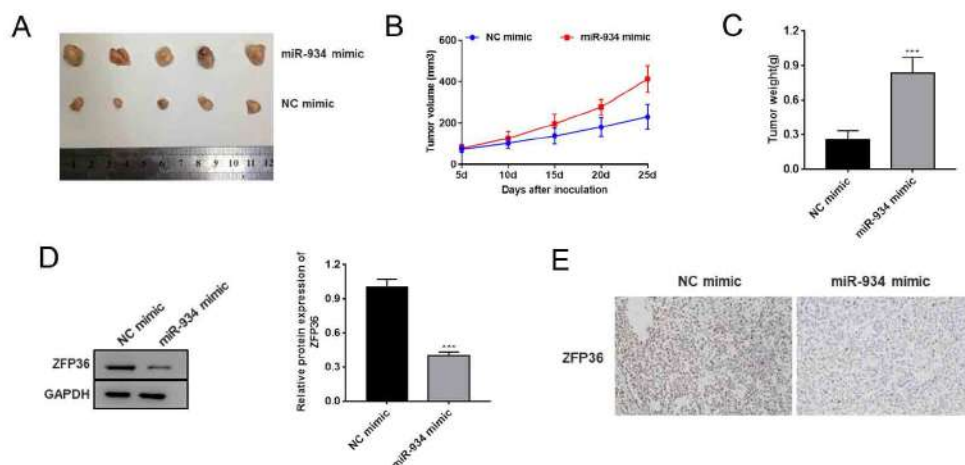


Fig. 5: miR-934 accelerated tumor growth *in vivo*. (A) AGS cells were used to induce xenografts in the nude mice. The xenografts were resected after 25 days of induction. (B) Tumor volumes were calculated after 5, 10, 15, 20 and 25 days of inoculation according to the formula: $(L \times S^2)/2$. L, long diameter; S, short diameter. (C) Tumor weights were measured after the xenografts were resected. (D) The protein expressions of ZFP36 were detected in the xenografts. (E) ZFP36-positive cells of the xenograft sections were stained by IHC assay. Each assay was repeated thrice. *** $P < 0.001$. NC, negative control; IHC, immunohistochemistry

Discussion

The imbalance between the expressions of oncogenes and tumor suppressor genes is the root cause of GC. Numerous miRNAs have been revealed to downregulate tumor suppressor genes and further promote cell proliferation, migration and invasion as oncogenes (29). In the current investigation, miR-934 was first reported to be upregulated in GC, and it positively regulated the tumorigenic behaviors of GC cells through inhibiting its target gene, ZFP36, bringing clinical significance for the diagnosis and treatment of GC. The previous cancer-related researches on miR-934 generally indicate miR-934 as an oncogene. For example, as an intronic miRNA of VGLL1, miR-934 was observably upregulated in estrogen receptor (ER)-negative breast carcinomas in accordant with VGLL1 (30). Alcohol-induced dysregulation of miR-934 activated the anti-apoptotic gene BCL-2 and promoted cell growth of head and neck squamous cell carcinoma (HNSCC) cell lines, which contributed to alcohol-associated HNSCC pathogenesis and progression (31). miR-934 promoted bladder cancer cell growth and xenograft tumor growth by binding to UBE2N, and the downregulated UBE2N

caused CDK6 protein accumulation, therefore accelerating tumor growth (32). Advanced pancreatic cancer was linked to higher level of miR-934; furthermore, cell migration and invasion of pancreatic cancer cells were positively regulated by miR-934/PROX1 axis (22). Despite miR-934 has been researched in various common tumors, its role is still not reported in GC. Herein, we evaluated the clinical tissues and GC cell lines and elucidated that miR-934 was markedly upregulated in GC. Besides, the cellular functional experiments revealed that miR-934 promoted cell growth and metastasis, while inhibition of miR-934 showed anti-tumor effects. The target gene of miR-934 was confirmed to be ZFP36. These findings took insight into the pathology of GC and suggested a novel target of targeted therapy for GC.

After the oncogenic role of miR-934 was identified in GC, we used bioinformatics approach to ulteriorly explore its target gene and ZFP36 Ring Finger Protein (ZFP36) was selected for the following research. ZFP36, also known as TTP, is involved in a large amount of malignancies. For example, in breast cancer, ZFP36 was negatively regulated by miR-423. Also, ZFP36 served as the target gene of circRNA_000554/miR-182 axis in

breast cancer. Upregulation of circRNA_000554 promoted ZFP36 expression to attenuate the progression of EMT in breast cancer (33). miR-513a-5p (34) was other identified upstream inhibitor of ZFP36 in breast cancer. Except for acting as target gene, ZFP36 could also bind to RNAs to impact the cellular functions of tumor cells. ZFP36 stabilized NBPF4 via the binding relationship, thus assisting NBPF4 to escape from inhibition by miR-17-3p, which ameliorated colorectal cancer (35). In our present study, we proved that the protein level of ZFP36 was downregulated in GC tissues, which was in accordant with the previous studies (36, 37). As the target of miR-934, the protein level of ZFP36 was negatively regulated by miR-934 and overexpression of ZFP36 partially ameliorated the carcinogenic effects of miR-934.

Conclusion

miR-934 promoted GC progression via targeting ZFP36, suggesting essential biomarkers for GC diagnosis and providing potential therapeutic axis for GC.

Journalism Ethical considerations

Ethical issues (Including plagiarism, informed consent, misconduct, data fabrication and/or falsification, double publication and/or submission, redundancy, etc.) have been completely observed by the authors.

Acknowledgements

No funding was received in this study.

Conflict of Interest

The authors declare that there is no conflict of interest.

References

1. Johnston FM, Beckman M (2019). Updates on

- Management of Gastric Cancer. *Curr Oncol Rep*, 21: 67.
2. Siegel RL, Miller KD, Jemal A (2016). Cancer statistics, 2016. *CA Cancer J Clin*, 66: 7-30.
3. Karimi P, Islami F, Anandasabapathy S, Freedman ND, Kamangar F (2014). Gastric cancer: descriptive epidemiology, risk factors, screening, and prevention. *Cancer Epidemiol Biomarkers Prev*, 23: 700-713.
4. Group G, Oba K, Paoletti X, et al (2013). Role of chemotherapy for advanced/recurrent gastric cancer: an individual-patient-data meta-analysis. *Eur J Cancer*, 49: 1565-1577.
5. Zhang XY, Zhang PY (2017). Gastric cancer: somatic genetics as a guide to therapy. *J Med Genet*, 54: 305-312.
6. Hamashima C (2014). Current issues and future perspectives of gastric cancer screening. *World J Gastroenterol*, 20: 13767-13774.
7. Patel TH, Cecchini M (2020). Targeted Therapies in Advanced Gastric Cancer. *Curr Treat Options Oncol*, 21: 70.
8. Mishra S, Yadav T, Rani V (2016). Exploring miRNA based approaches in cancer diagnostics and therapeutics. *Crit Rev Oncol Hematol*, 98: 12-23.
9. Chen L, Heikkinen L, Wang C, Yang Y, Sun H, Wong G (2019). Trends in the development of miRNA bioinformatics tools. *Brief Bioinform*, 20: 1836-1852.
10. Bernardo BC, Ooi JY, Lin RC, McMullen JR (2015). Mirna therapeutics: a new class of drugs with potential therapeutic applications in the heart. *Future Med Chem*, 7: 1771-1792.
11. Lu TX, Rothenberg ME. MicroRNA (2018). *J Allergy Clin Immunol*, 141: 1202-1207.
12. Fabian MR, Sonenberg N (2012). The mechanics of miRNA-mediated gene silencing: a look under the hood of miRISC. *Nat Struct Mol Biol*, 19: 586-593.
13. Rupaimoole R, Slack FJ (2017). MicroRNA therapeutics: towards a new era for the management of cancer and other diseases. *Nat Rev Drug Discov*, 16: 203-222.
14. Wang C, Huang Y, Zhang J, Fang Y (2020). miRNA-339-5p suppresses the malignant development of gastric cancer via targeting ALKBH1. *Exp Mol Pathol*, 115: 104449.
15. Hu X, Zhang M, Miao J, Wang X, Huang C (2018). miRNA-4317 suppresses human gastric cancer cell proliferation by targeting

- ZNF322. *Cell Biol Int*, 42: 923-930.
16. Lin J, Shen J, Yue H, Cao Z (2019). miRNA1835p.1 promotes the migration and invasion of gastric cancer AGS cells by targeting TPM1. *Oncol Rep*, 42: 2371-2381.
 17. Liu B, Li J, Cairns MJ (2014). Identifying miRNAs, targets and functions. *Brief Bioinform*, 15: 1-19.
 18. Zhao YB, Zhao XY, Jia J, Liu J, Xu JL, Li N (2021). Up-regulation of miR-934 serves as an independent prognostic factor for lung cancer and promotes proliferation, migration and invasion of non-small cell lung cancer cells. *J Biol Regul Homeost Agents*, 35: 315-322.
 19. Zhao S, Mi Y, Guan B, et al (2020). Tumor-derived exosomal miR-934 induces macrophage M2 polarization to promote liver metastasis of colorectal cancer. *J Hematol Oncol*, 13: 156.
 20. Lu Y, Hu X, Yang X (2021). miR-934 promotes breast cancer metastasis by regulation of PIEN and epithelial-mesenchymal transition. *Tissue Cell*, 71: 101581.
 21. Liu W, Ma L, Zhang J (2021). MicroRNA-934 promotes colorectal cancer cell proliferation by directly targeting Dickkopf-related protein 2. *Exp Ther Med*, 22: 1041.
 22. Jin Y, Weng Y, Wang Y, et al (2020). miR-934 as a Prognostic Marker Facilitates Cell Proliferation and Migration of Pancreatic Tumor by Targeting PROX1. *Onco Targets Ther*, 13: 3389-3399.
 23. Hu Y, Zhang Q, Cui J, et al (2019). Oncogene miR-934 promotes ovarian cancer cell proliferation and inhibits cell apoptosis through targeting BRMS1L. *Eur Rev Med Pharmacol Sci*, 23: 5595-5602.
 24. Poh AR, O'Donoghue RJ, Ernst M, Putoczki TL (2016). Mouse models for gastric cancer: Matching models to biological questions. *J Gastroenterol Hepatol*, 31: 1257-1272.
 25. Chen W, Chen M, Zhao Z, et al (2020). ZFP36 Binds With PRC1 to Inhibit Tumor Growth and Increase 5-Fu Chemosensitivity of Hepatocellular Carcinoma. *Front Mol Biosci*, 7: 126.
 26. Selmi T, Martello A, Vignudelli T, et al (2012). ZFP36 expression impairs glioblastoma cell lines viability and invasiveness by targeting multiple signal transduction pathways. *Cell Cycle*, 11: 1977-1987.
 27. Xia W, Liu Y, Du Y, Cheng T, Hu X, Li X (2020). MicroRNA-423 Drug Resistance and Proliferation of Breast Cancer Cells by Targeting ZFP36. *Onco Targets Ther*, 13: 769-782.
 28. Pan QH, Fan YH, Wang YZ, Li DM, Hu CE, Li RX (2020). Long noncoding RNA NNT-AS1 functions as an oncogene in breast cancer via repressing ZFP36 expression. *J Biol Regul Homeost Agents*, 34: 795-805.
 29. Shin VY, Chu KM (2014). miRNA as potential biomarkers and therapeutic targets for gastric cancer. *World J Gastroenterol*, 20: 10432-10439.
 30. Castilla MA, Lopez-Garcia MA, Atienza MR, et al (2014). VGLL1 expression is associated with a triple-negative basal-like phenotype in breast cancer. *Endocr Relat Cancer*, 21: 587-599.
 31. Saad MA, Kuo SZ, Rahimy E, et al (2015). Alcohol-dysregulated miR-30a and miR-934 in head and neck squamous cell carcinoma. *Mol Cancer*, 14: 181.
 32. Yan H, Ren S, Lin Q, et al (2019). Inhibition of UBE2N-dependent CDK6 protein degradation by miR-934 promotes human bladder cancer cell growth. *FASEB J*, 33: 12112-12123.
 33. Mao Y, Lv M, Cao W, et al (2020). Circular RNA 000554 represses epithelial-mesenchymal transition in breast cancer by regulating microRNA-182/ZFP36 axis. *FASEB J*, 34: 11405-11420.
 34. Fang S, Zhao Y, Hu X (2020). LncRNA ADAMTS9-AS1 Restrains the Aggressive Traits of Breast Carcinoma Cells via Sponging miR-513a-5p. *Cancer Manag Res*, 12: 10693-10703.
 35. Chen W, Di Z, Chen Z, et al (2021). NBPf4 mitigates progression in colorectal cancer through the regulation of EZH2-associated ETFA. *J Cell Mol Med*, 25: 9038-9050.
 36. Wang H, Chen Y, Guo J, et al (2018). Dysregulation of tristetraprolin and human antigen R promotes gastric cancer progressions partly by upregulation of the high-mobility group box 1. *Sci Rep*, 8: 7080.
 37. Guo J, Qu H, Shan T, Chen Y, Chen Y, Xia J (2018). Tristetraprolin Overexpression in Gastric Cancer Cells Suppresses PD-L1 Expression and Inhibits Tumor Progression by Enhancing Antitumor Immunity. *Mol Cells*, 41: 653-664.